J. Membrane Biol. 163, 97–110 (1998)

The Journal of
Membrane
Biology

Separate Swelling- and Ca^{2+}-activated Anion Currents in Ehrlich Ascites Tumor Cells

S.F. Pedersen[1], J. Prenen[2], G. Droogmans[2], E.K. Hoffmann[1], B. Nilius[2]

[1]Department of Biochemistry, August Krogh Institute, University of Copenhagen, Denmark
[2]KU Leuven, Laboratorium voor Fysiologie, Campus Gasthuisberg, B-3000 Leuven, Belgium

Received: 12 November 1997/Revised: 5 February 1998

Abstract. A Ca^{2+}-activated ($I_{Cl,Ca}$) and a swelling-activated anion current ($I_{Cl,vol}$) were investigated in Ehrlich ascites tumor cells using the whole cell patch clamp technique. Large, outwardly rectifying currents were activated by an increase in the free intracellular calcium concentration ($[Ca^{2+}]_i$), or by hypotonic exposure of the cells, respectively. The reversal potential of both currents was dependent on the extracellular Cl^- concentration. $I_{Cl,Ca}$ current density increased with increasing $[Ca^{2+}]_i$, and this current was abolished by lowering $[Ca^{2+}]_i$ to <1 nM using 1,2-bis-(o-aminophenoxy)ethane-N,N,N′,N′-tetra-acetic acid (BAPTA). In contrast, activation of $I_{Cl,vol}$ did not require an increase in $[Ca^{2+}]_i$. The kinetics of $I_{Cl,Ca}$ and $I_{Cl,vol}$ were different: at depolarized potentials, $I_{Cl,Ca}$ as activated in a $[Ca^{2+}]_i$- and voltage-dependent manner, while at hyperpolarized potentials, the current was deactivated. In contrast, $I_{Cl,vol}$ exhibited time- and voltage-dependent deactivation at depolarized potentials and reactivation at hyperpolarized potentials. The deactivation of $I_{Cl,vol}$ was dependent on the extracellular Mg^{2+} concentration. The anion permeability sequence for both currents was $I^- > Cl^- >$ gluconate. $I_{Cl,Ca}$ was inhibited by niflumic acid (100 μM), 5-Nitro-2-(3-phenylpropylamino)benzoic acid (NPPB, 100 μM) and 4,4′-diisothiocyano-2,2′-stilbenedisulfonic acid (DIDS, 100 μM), niflumic acid being the most potent inhibitor. In contrast, $I_{Cl,vol}$ was unaffected by niflumic acid (100 μM), but abolished by tamoxifen (10 μM). Thus, in Ehrlich cells, separate chloride currents, $I_{Cl,Ca}$ and $I_{Cl,vol}$, are activated by an increase in $[Ca^{2+}]_i$ and by cell swelling, respectively.

Key words: Patch clamp — Ca^{2+}- and voltage-dependence — Regulatory Volume Decrease — Tamoxifen — Niflumic acid — Mg^{2+}

Correspondence to: B. Nilius

Introduction

The swelling-induced activation of separate K^+ and Cl^- channels as a mechanism for Regulatory Volume Decrease (RVD) was first proposed for Ehrlich ascites tumor cells (Hoffmann, 1978). The resulting loss of KCl and osmotically obliged water is the main mechanism of RVD in most cell types (*see* Hoffmann & Dunham, 1995). An increase in $[Ca^{2+}]_i$ likewise activates conductive pathways for transport of K^+ and Cl^- in Ehrlich ascites tumor cells, leading to loss of KCl and concomitant cell shrinkage (Hoffmann, Lambert & Simonsen, 1986). The membrane potential is depolarized in hypotonically swollen cells because the increase in Cl^- conductance exceeds the increase in K^+ conductance, whereas it is hyperpolarized after an increase in $[Ca^{2+}]_i$, because the increase in K^+ conductance exceeds the increase in Cl^- conductance under these conditions (Lambert, Hoffmann & Jørgensen, 1989).

The nature of the volume- and Ca^{2+}-activated channels was previously studied at the single channel level in the cell attached mode (Christensen & Hoffmann, 1992). Cell swelling was found to activate a 2-7 pS Cl^- channel in an all-or-none fashion. The activity of this channel was insensitive to Ca^{2+} in excised patches. In intact cells, a 7 pS channel was observed, which could also be activated in cell-attached patches when the Ca^{2+}-ionophore A23187 was added to the medium. From the single channel measurements performed by Christensen and Hoffmann (1992), it could not be determined whether this channel was different from the volume-activated channel. Ca^{2+}-activated Cl^- channels have been described in various studies on excitable and nonexcitable cells (Cliff & Frizzell, 1990; Arreola, Melvin & Begenisich, 1996; Nilius et al., 1997*a,b;* for reviews *see* Valverde, Hardy & Sepúlveda, 1995; Jentsch, 1996; Nilius, Viana & Droogmans, 1997*c*). ''Mini'' Cl^- channels activated by cell swelling have been described at the whole

cell level in bovine chromaffin cells (Doroshenko & Neher, 1992), neutrophils (Stoddard, Steinbach & Simchowitz, 1993), human endothelial cells (Nilius et al., 1994), and human T-lymphocytes (Schumacher et al., 1995; for reviews, *see* Valverde et al., 1995; Jentsch 1996; Strange, Emma & Jackson, 1996; Nilius et al., 1996; 1997*b*,*d*). Whether these channels represent the same channel as those described in Ehrlich cells is unclear. It has recently been suggested that the single channel conductances obtained in the above-mentioned studies using stationary noise analysis might be underestimated at least 15-fold (for a discussion, *see* Strange et al., 1996). If this is correct, these Cl^- channels might be of the larger VSOAC type (*see* Strange et al., 1996) rather than of the Ehrlich cell type, for which the small single channel conductance was obtained directly by single channel measurements. Anion currents activated by cell swelling have not yet been characterized at the whole cell level in Ehrlich cells, and their possible identity with volume-activated Cl^- channels described in other cells is thus difficult to evaluate. This is a key question, which needs to be addressed for several reasons. Firstly, Ehrlich cells seem to be unusual compared to most other cell types studied in that efflux of taurine and Cl^-, which in most cells is suggested to be mediated via the same channel, appears to occur predominantly via separate channels in Ehrlich cells (Lambert & Hoffmann, 1994). Secondly, the mechanisms leading to swelling-induced activation of Cl^- channels seems to vary between cell types, and it remains unclear whether the apparent differences in the regulation of $I_{Cl,vol}$ reflect the expression of different types of volume sensitive anion channels in different cell types. In Ehrlich cells, a role for leukotriene D_4 (LTD_4) in the swelling-induced Cl^- channel activation has been suggested, possibly involving a direct effect of LTD_4 on the channel (*see* Hoffmann & Dunham, 1995). In rat hepatoma cells, the swelling-induced activation of whole cell Cl^- currents was proposed to involve release of ATP and autocrine stimulation of P_2-purinoceptors (Wang et al., 1996). In guinea pig cardiac myocytes, the Cl^- channel activated by β-adrenergic receptors ($I_{Cl,cAMP}$) was suggested to be involved in the RVD process (Wang et al., 1997). While the swelling-induced activation of Cl^- channels usually does not require an increase in $[Ca^{2+}]_i$ (*see* Nilius et al., 1997*b*), an increase in $[Ca^{2+}]_i$ has ben proposed to be required for activation of the RVD response in some cell types, but not in others (*see* Hoffmann & Dunham, 1995). In Ehrlich cells, an increase in $[Ca^{2+}]_i$ can be detected in only 6% of the cells during RVD (Jørgensen et al., 1997).

The purpose of the present study was to characterize the currents elicited by increases in $[Ca^{2+}]_i$ and by cell swelling, respectively, in Ehrlich cells, in order to evaluate whether these currents are mediated by different channels in these cells, and whether they resemble channels previously described in other cell types.

Materials and Methods

Cell Suspensions and Solutions

The Ehrlich ascites tumor cells (hyperdiploid strain) were maintained in white NMRI mice by weekly intraperitoneal transplantation. Cells for experimental use were harvested 6–8 days after transplantation and suspended at a cytocrit of 0.2–0.5% in a modified Krebs solution of the following composition (mM): 150 NaCl, 6 KCl, 1.5 $CaCl_2$, 1 $MgCl_2$, 10 HEPES, 10 glucose. The pH was adjusted to 7.4 with NaOH. The osmolarity of the media was 315 ± 5 mOsm, measured using a Wescor 5500 vapor pressure osmometer (Schlag Instruments, Gladbach, Germany).

$I_{Cl,Ca}$: In order to suppress inward K^+- and Na^+-currents, KCl was omitted from the bath solution, and this solution contained only 10 Na^+ (NaCl substituted for equimolar amounts of NMDG-Cl). In anion selectivity experiments, NaCl was substituted by equimolar amounts of NaI or Na-gluconate. The Ca^{2+}-buffered pipette solutions contained (mM): 40 CsCl, 100 Cs-apartate, 1 $MgCl_2$, 4 Na_2ATP, 10 HEPES, 5 EGTA, and the amount of $CaCl_2$ required to adjust the free Ca^{2+} concentration to 25, 100, 250, and 500 nM, respectively (calculated using the program CaBuf, G. Droogmans). In the BAPTA pipette solution, $CaCl_2$ and EGTA were omitted, and 5 BAPTA (as pentapotassium salt or free acid) was added. The pH of the pipette solution was adjusted to 7.2 with CsOH. The osmolarity of the pipette solution was 290 ± 5 mOsm, i.e., about 25 mOsm hypotonic compared to the external solutions, in order to avoid activation of volume sensitive Cl^- currents.

$I_{Cl,vol}$: Before the hypotonic exposure, the Ehrlich cells were perfused with an isosmotic solution of the following composition (mM): 86.3 NaCl, 6 KCl, 1.5 $CaCl_2$, 1 $MgCl_2$, 10 HEPES, 10 glucose, 129 mannitol. The osmolarity of this solution was 324 ± 8.2 mM. The hypotonic solutions (13% = 282 mOsm, 27% = 237 mOsm, and 40% = 194 mOsm) were prepared by adjusting the amount of mannitol in the solution. For anion selectivity experiments, modified 40% hypotonic solutions were prepared by substitution of NaCl by equimolar amounts of NaI or Na-gluconate. The pH of all these solutions was adjusted to 7.4 with NaOH. The pipette solution contained (mM): 40 CsCl, 100 Cs-apartate, 1 $MgCl_2$, 4 Na_2ATP, 10 HEPES, 10 BAPTA, and 1.63 $CaCl_2$, resulting in a free Ca^{2+} concentration of 25 nM (calculated using the program CaBuf, G. Droogmans). The pH of the pipette solution was adjusted to 7.2 with CsOH. The osmolarity of the pipette solution was approximately 295 mOsm. In experiments in which the bath Mg^{2+} concentration was increased, this was performed by replacing NMDG-Cl with $MgCl_2$, in order to maintain a constant Cl^- concentration.

Whole Cell Recording

Whole cell currents were measured essentially as previously described in detail (Nilius et al., 1994). Briefly, the Ehrlich cells were allowed to settle on poly-L-lysine coated (0.1 mg/ml, Sigma) glass coverslips and mounted on the stage of a Zeiss Axiovert 100 microscope. Currents were monitored using an EPC-7 patch clamp amplifier (List Electronic, Germany) and sampled at 2 msec intervals. For anion substitution experiments, an agar bridge electrode was employed. The cells were continuously perfused using a fast perfusion system. Pipette resistance was 3-5 MΩ. The holding potential was −50 mV. The following voltage protocol was used in most experiments, and was applied every 15 seconds: a 600 msec step to −80 mV, a 200 msec step to −100 mV, followed by a 2.6 sec linear voltage ramp to +100 mV. Other voltage protocols are described in the figure legends. All experiments were

performed at room temperature (20–23°C). The cell capacitance was used as an estimate of cell surface area, and hence, cell size. Patch clamp data were analyzed using in-house software (WinASCD, Guy Droogmans). Corrections for junction potential (*see* Neher, 1992) were calculated using Axoscope software. Under the conditions used in the present study, currents recorded under isotonic conditions were very small and were not subtracted prior to analysis of the data.

Chemicals

Unless otherwise indicated, chemicals were obtained from Sigma, Fluka Chemie AG (Buchs, Switzerland), or Merck (Darmstadt, Germany). Fura-2-AM (TEFLABS, Austin, Texas) was prepared as a 1 mM stock in DMSO. NPPB (Research Biochemicals International, Natick, MA), DIDS and Niflumic acid (Sigma Chemical, Saint Louis, MO) were prepared as 100 mM stock solutions in DMSO (final DMSO concentration 0.1%). Tamoxifen was prepared as a 10 mM stock solution in methanol. These solutions were kept at −20°C until use. Other inorganic salts were obtained from Sigma, Fluka Chemie AG (Buchs, Switzerland), or Merck (Darmstadt, Germany).

Measurement of $[Ca^{2+}]_i$

$[Ca^{2+}]_i$ was measured as described in Nilius et al. (1994).

Data analysis and Statistical Evaluation

The percent inhibition of $I_{Cl,Ca}$ by the Cl^- channel blockers was calculated as (Eq. 1)

$$\%\ inhibition = \frac{I_{ctrl} - I_X}{I_{ctrl}}\ 100\% \qquad (1)$$

where I_x is the current magnitude in nA measured at +100 mV in the presence of the inhibitor, I_{ctrl} is the mean of the current magnitudes measured before application and after removal of the inhibitor, respectively.

The dependence of $I_{Cl,vol}$ on the magnitude of the hypotonic challenge was evaluated as the current magnitude measured in a small window at +100 mV and −80 mV, at time 1.5 min after start of the hypotonic perfusion.

The percent inhibition of $I_{Cl,vol}$ in the presence of niflumic acid or tamoxifen was calculated as the difference between the mean current magnitude, measured at +100 mV in the interval 1.5–2 min after start of the hypotonic perfusion, in the absence and presence of the inhibitor, in percent of that measured in the absence of the inhibitor (hypotonic control conditions).

The shifts in V_{rev} were used to calculate the permeabilities of the various anions relative to that of Cl^-, using the modified Goldman-Hodgkin-Katz equation (Eq. 2)

$$P_X/P_{Cl} = ([Cl^-]_o \exp(-\Delta V_{rev} F/RT) - [Cl^-]_s)/[X^-]_o \qquad (2)$$

where $[Cl^-]_o$ is the Cl^- concentration in the standard medium, $[Cl^-]_s$ and $[X^-]_o$ are the concentrations of Cl^- and the substituting anion in the substituted medium, respectively, ΔV_{rev} is the measured shift in reversal potential, and *F*, *R* and *T* have their usual meanings.

The $V_{rev,calc}$ was estimated taking into account the relative permeabilities of the channel to gluconate and aspartate, as (Eq. 3)

$$V_{rev} = \frac{RT}{F} \cdot \ln \frac{P_{Cl} \cdot [Cl]_i + P_{Asp} \cdot [Asp]_i}{P_{Cl} \cdot [Cl]_o + P_{Gluc} \cdot [Gluc]_o} \qquad (3)$$

where $[Cl]_i$, $[Asp]_i$, $[Cl]_o$ and $[Gluc]_o$ are the concentrations of these anions in the pipette and bath solutions, respectively, and *F*, *R* and *T* have their usual meanings. Results are presented as means ± SEM, with the number of cells in parenthesis, or as single experiments representative of data from at least 4 experiments (data from at least 3 mice). Significance was tested using a Student's *t*-test (level of significance: $P < 0.05$).

Abbreviations:

BAPTA: 1,2-bis-(o-aminophenoxy) ethane-N,N,N′,N′-tetraacetic acid; $[Ca^{2+}]_i$: the free, intracellular calcium concentration; DIDS: 4,4′-diisothiocyano-2,3′-stilbenedisulfonic acid; DMSO: dimethylsulfoxide; EGTA: ethylene glycol-bis-(β-aminoethylether)-N,N,N′,N′, tetraacetic acid; HEPES: N-(2-hydroxyethyl) piperazine-N′-2-ethanesulfonic acid; NMDG: N-methyl-D-glucamine; NPPB: 5-Nitro-2-(3-phenylpropylamino)benzoic acid.

Results

Activation of a Whole Cell Current by an Increase in the Free Intracellular Calcium Concentration ($[Ca^{2+}]_i$)

The current was activated by dialyzing the Ehrlich cell, via the patch pipette, with solutions of known free calcium concentrations ($[Ca^{2+}]$), buffered with EGTA. This resulted in rapid loading of these relatively small cells (10–20 pF) with Ca^{2+} (*data not shown*) and the concomitant activation of an outwardly rectifying whole cell current. The properties of the Ca^{2+}-activated current were investigated by stepping the voltage from the holding potential of −50 mV to potentials from −80 to +140 mV. Figure 1*A* shows current traces obtained using this protocol, at a $[Ca^{2+}]_i$ of 100 nM. As seen, the recorded current usually consisted of a time-independent component and a component, which slowly activated at positive potentials, and deactivated upon return to the holding potential. Figure 1*B* shows the corresponding current-voltage (*IV*) relationship, obtained from currents measured in a narrow window at the point indicated by the arrow in Fig. 1*A*. As seen, the steady-state current showed strong outward rectification. The reversal potential (V_{rev}) of the activated current, as measured from currents during voltage ramps, was −11.5 ± 1.3 mV ($n = 21$). The junction potential between the bath- and pipette solutions under the present experimental conditions can be calculated at −19 mV (*see* Neher, 1992), hence, the actual current reversal potential is estimated at −30.5 mV, close to the calculated reversal potential of −29 mV for a Cl^- current under these conditions. The kinetics of the deactivation of the Ca^{2+}-activated current were examined using the following protocol: A 1-sec step to +140 mV was applied to fully activate the current, followed by voltage steps ranging from +120 to −80 mV. The current appeared to decay rapidly at negative poten-

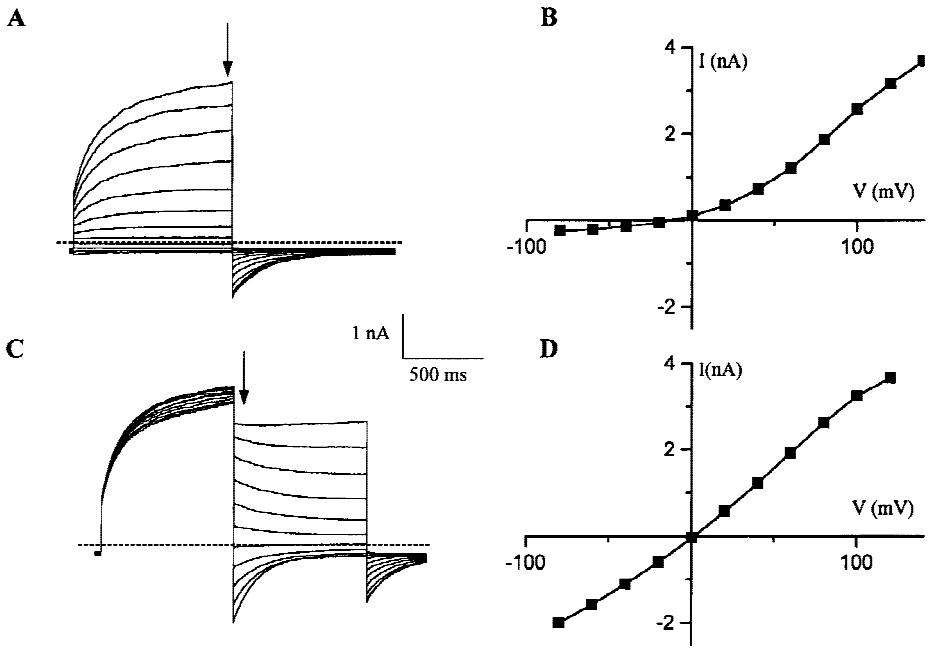

Fig. 1. Activation of an outwardly rectifying current by an increase in $[Ca^{2+}]_i$. (*A*) Current traces generated after loading the cell with 100 nM free Ca^{2+} via the patch pipette. From a holding potential of −50 mV, 20-mV steps of 1-sec duration were applied from +140 to −80 mV. The time between episodes was 5 sec. The extracellular solution was a modified Krebs solution in which KCl was omitted, and 130 of the 140 mM NaCl was replaced with NMDG-Cl, to reduce contributions from K^+- and nonselective currents to the whole cell currents (*see* Materials and Methods). The cell capacitance was 12 pF. The arrow marks the point used to construct *IV* relationship shown in *B*. Note that the current activates slowly at positive potentials, and inactivates rapidly upon return to the holding potential. The figure is representative of experiments on 12 cells under the same conditions. (*B*) Same cell and conditions as in *A*. *IV* relationship generated at 100 nM $[Ca^{2+}]_i$, from the current traces shown in *A*. The average current in a small window indicated by the arrow in *A* was calculated at each potential. Note the strong outward rectification of the Ca^{2+}-activated current, which is due to inactivation of the current at negative potentials. (*C*) Same cell and conditions as in *A*. From the holding potential of −50 mV, a 1-sec voltage step to +140 mV was applied, followed by 1-sec step to potentials ranging from +120 to −80 mV, at intervals of 20 mV. The arrow marks the interval used to construct the instantaneous *IV* relationship shown in *D*. Note the deactivation of the current at negative potentials. The figure is representative of experiments on 9 cells under the same conditions. (*D*) *IV* relationship generated at 100 nM $[Ca^{2+}]_i$, from the current traces in *C*. The average current in a small window indicated by the arrow in *C* was calculated at each potential. Compare the linearity of the instantaneous *IV* relationship to the strong outward rectification of the steady state current (panel *B*).

tials and more slowly at the more positive potentials (Fig. 1*C*). Figure 1*D* shows the *IV* relationship obtained in a narrow window at the point indicated by the arrow in Fig. 1*C*. In contrast to the steady-state current, the instantaneous current-voltage relationship (Fig. 1*D*) as obtained after full activation of the current by a voltage step to +140 mV, was almost linear.

Ca^{2+} Dependence of the Current Magnitude

The magnitude of the current activated was strongly dependent on the free Ca^{2+} concentration of the internal solution. Figure 2*A* shows representative whole cell currents recorded at various $[Ca^{2+}]_i$, and normalized to cell capacitance. When intracellular Ca^{2+} was chelated by adding 5 mM BAPTA to the pipette solution and omitting $CaCl_2$, these currents were completely abolished. A very small current was observed with 25 nM free Ca^{2+} in the pipette, and as $[Ca^{2+}]_i$ was further increased to 100, 250 and 500 nM, current magnitude increased, apparently saturating around 250 nM free Ca^{2+} (Fig. 2*B*). As seen, the current density was substantial, reaching 102 ± 27 pA pF^{-1} ($n = 12$) at a $[Ca^{2+}]_i$ of 100 nM, and 206 ± 45 ($n = 10$) at a $[Ca^{2+}]_i$ of 500 nM, at a holding potential of +100 mV.

Ca^{2+} Dependence of the Current Kinetics

The kinetics of activation and deactivation of the Ca^{2+}-activated current were further investigated using the step protocols described above. Activation and deactivation of the current were both well fitted by a sum of two exponentials and a time-independent component. The time constant ($\tau_{slow,act}$) of the slow component was in the range of 2–3 seconds, with an amplitude of about 1–2 nA (*data not shown*). Since a careful analysis of this component would require excessively long voltage steps, this component was omitted from the further analysis. Fig-

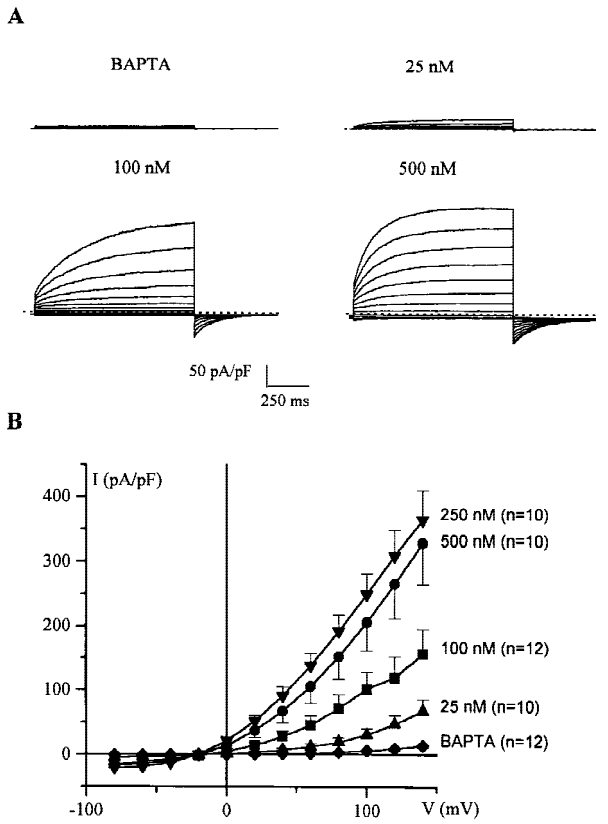

Fig. 2. Current dependence on $[Ca^{2+}]_i$. (*A*) Current traces obtained during voltage step protocols. The extracellular solution was a modified Krebs solution in which KCl was omitted, and 130 of the 140 mM NaCl was replaced with NMDG-Cl. The pipette solution contained either 5 mM BAPTA and no $CaCl_2$, or 5 mM EGTA and the amount of $CaCl_2$ required to adjust $[Ca^{2+}]_i$ to the desired value (*see* Materials and Methods). The voltage step protocol was as described in Fig. 1*A*. The traces are representative of 10–12 experiments for each $[Ca^{2+}]_i$. (*B*) Mean *IV* relationships at varying values of $[Ca^{2+}]_i$, calculated from current traces as shown in *A*.

ure 3*A* shows the fast time constant of current activation ($\tau_{fast,act}$) as a function of the applied potential, and at various values of $[Ca^{2+}]_i$. As seen, $\tau_{fast,act}$ was clearly voltage-dependent, being faster at the more positive potentials. Furthermore, at the less positive potentials, $\tau_{fast,act}$ was dependent on $[Ca^{2+}]_i$, with the fastest time constants obtained at high $[Ca^{2+}]_i$. Figure 3*B* shows the fast time constant of current deactivation ($\tau_{fast,deact}$) as a function of the applied potential, and at various values of $[Ca^{2+}]_i$. As seen, in contrast to $\tau_{fast,act}$, $\tau_{fast,deact}$ appeared to be largely independent of $[Ca^{2+}]_i$ and holding potential.

A Hypotonic Challenge Activates an Outwardly Rectifying Cl^- Current, $I_{Cl,vol}$

A hypotonic challenge in the presence of 1 mM extracellular Ca^{2+} will elicit a detectable increase in the free intracellular Ca^{2+} concentration ($[Ca^{2+}]_i$) in 6% of the Ehrlich cells (Jørgensen et al., 1997). Thus, to avoid activation of $I_{Cl,Ca}$ during cell swelling, the free Ca^{2+} concentration in the pipette was always buffered with 10 mM BAPTA at 25 nM. Under these conditions, perfusion of the cells with a 27% hypotonic solution resulted in visible cell swelling and, within 1–2 min, development of an outwardly rectifying membrane current. Figure 4*A* shows the time course of the current measured in a small window at +100 and −80 mV, respectively, in an experiment in which an Ehrlich cell was repetitively exposed to a 27% hypotonic solution. Panel *B* shows the *IV* relationship at various time points during the experiment, as indicated in *A*. From *IV* curves such as those shown in Fig. 4*B*, V_{rev} of the swelling-activated current could be measured at −5.8 ± 0.50 ($n = 13$). The junction potential between the bath- and pipette solutions under these conditions was calculated at −13 mV, hence, when corrected for the junction potential, V_{rev} is very close to the calculated equilibrium potential for a Cl^--selective channel (−19 mV). As seen in Fig. 4*C*, the current could be reduced by perfusion with a hypertonic solution, supporting the notion that it was cell volume dependent.

Voltage-dependent Properties of $I_{Cl,vol}$

The voltage-dependent properties of the swelling-activated current were studied by changing the voltage in a stepwise manner from the holding potential of −50 mV, as shown in Fig. 5. The recorded current exhibited a characteristic time-dependent deactivation at positive potentials, similar to that described for swelling-activated anion currents in other cell types (Jackson & Strange, 1995; Voets et al., 1997). Figure 5*A* also shows that no tail currents could be observed upon return to the holding potential. This is in contrast to the prominent tail currents characteristic of $I_{Cl,Ca}$ (*see* Fig. 1*A*). Figure 5*B* shows *IV*-relationships calculated from the step protocols shown in *A*. Under isotonic conditions, the whole cell current is seen to be virtually zero. The swelling-activated current is clearly outward rectifying at the beginning of the voltage step (*a*), whereas it flattens of at the end of the 1-sec voltage steps (*b*), due to the voltage-dependent current deactivation. Figure 5*C* shows an experiment investigating the effect of hyperpolarizing potentials on the deactivated current. The current was stepped to +140 mV for 1 sec to elicit channel inactivation. This was followed by 2-sec steps to voltages ranging from +120 to −80 mV. As seen, membrane hyperpolarization induced a slight current reactivation, which appeared to be faster at the more hyperpolarized potentials ($n = 8$). This was not further investigated in the present study (*see*, however, Discussion).

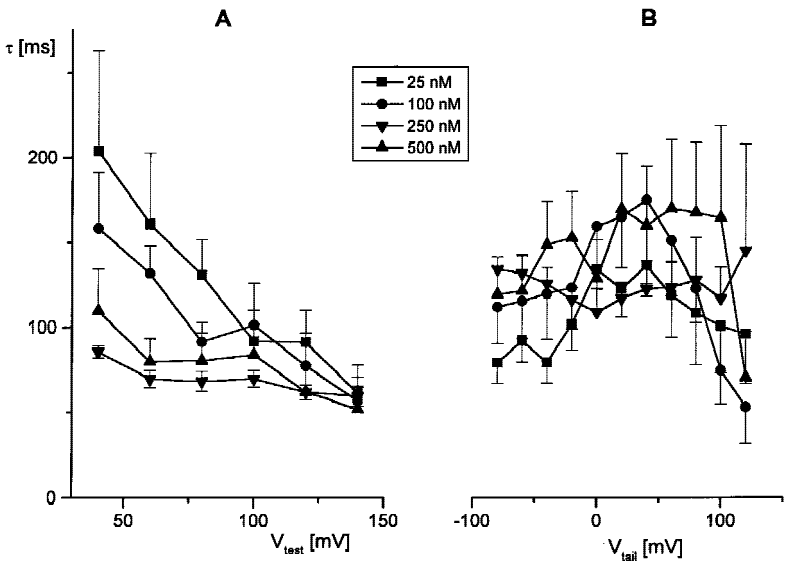

Fig. 3. Dependence of current kinetics on voltage and $[Ca^{2+}]_i$. (*A*) Fast time constants of current activation at varying voltage and $[Ca^{2+}]_i$, obtained from double exponential fits to current traces. The equation used to fit the current traces was of the form: $I(t) = A_{ss} + A_{fast} \exp(-t/\tau_{fast}) + A_{slow} \exp(-t/\tau_{slow})$. The experimental conditions and voltage step protocol were as in Fig. 1*A*. Data shown are means ± SEM from 10 cells at each $[Ca^{2+}]_i$. As seen, current activation is faster at more depolarized potentials and at higher $[Ca^{2+}]_i$. Slow time constants appeared to be voltage-independent, but were too slow to be evaluated using the present experimental protocol (*data not shown*). (*B*) Fast time constants of current deactivation at varying voltage and $[Ca^{2+}]_i$, obtained from double exponential fits to current traces. The experimental conditions and voltage step protocol were as in Fig. 1*C*. Data shown are means ± SEM from 9–10 cells at each $[Ca^{2+}]_i$. As seen, τ_{fast} appears to be largely $[Ca^{2+}]_i$- and voltage-independent. Similar to those of current activation, slow time constants of deactivation appeared to be voltage-independent, but were too slow to be evaluated using the present experimental protocol (*data not shown*).

Time Course and Magnitude of $I_{Cl,vol}$ is Dependent on the Magnitude of the Hypotonic Challenge

The time course of current activation, as well as the magnitude of the current, was dependent on the magnitude of the hypotonic challenge. This is illustrated in Fig. 6. Figure 6*A* shows the current monitored over time at +100 and −80 mV, respectively, under isotonic conditions and during exposure of the cell to hypotonic challenges of 13% and 40%, respectively. Figure 6*B* shows current traces obtained using the 1-sec voltage step protocol, at the time indicated in *A.* These data are summarized in Fig. 6*C*, which shows the current density recorded at +100 and −80 mV at time 1 min after hypotonic exposure. The 1-min time point was used for comparison of the degree of current activation, since the currents continued to increase during the hypotonic challenge, preventing comparison of maximal current densities. The current densities obtained at a holding potential of +100 mV were 15 ± 4.5 pA/pF ($n = 5$), 38 ± 7.3 pA/pF ($n = 7$) and 65 ± 8.2 ($n = 7$) at 13%, 27% and 40% hypotonic challenges, respectively, compared to 10 ± 2.8 pA/pF under isotonic conditions ($n = 10$). As seen, the current density reached after 1 min of hypotonicity is directly correlated to the magnitude of the hypotonic challenge.

Kinetics of the Voltage-Dependent Inactivation of $I_{Cl,vol}$

The kinetics of the voltage-dependent deactivation of $I_{Cl,vol}$ were further investigated using long (>2500 msec) duration voltage steps from −80 to +120 mV. At voltages above ~60 mV, current deactivation was observed in most cells. The rate and magnitude of deactivation of $I_{Cl,vol}$ increased with increasing depolarization, sometimes resulting in crossing-over of the currents at the most depolarized potentials. The time course of current deactivation was best fitted by a double exponential function. The fast (τ_{fast}) and slow (τ_{slow}) time-constants of deactivation were found to be voltage-dependent, both decreasing with increasing depolarization. The magnitude of τ_{fast} decreased from 312 ± 74 msec at +60 mV to 153 ± 62 msec at +120 mV, whereas that of τ_{slow} decreased from 2097 ± 666 msec at +60 mV to 1075 ± 267 msec at +120 mV.

Effect of the Extracellular Mg^{2+} Concentration ($[Mg^{2+}]_o$) on Voltage-dependent Inactivation of $I_{Cl,vol}$

Recently, acceleration of the voltage-dependent deactivation of $I_{Cl,vol}$ by increasing concentrations of extracellular divalent cations was reported in studies on cervical carcinoma cells (Anderson, Jirsch & Fedida, 1995) and BC_3H1 myoblasts (Voets, Droogmans & Nilius, 1997). Thus, we investigated the effect of increasing $[Mg^{2+}]_o$ on the deactivation kinetics of $I_{Cl,vol}$ in Ehrlich cells. The results of these experiments are shown in Fig. 7. Panel *A* shows a series of current traces obtained from the same cell by applying 1-sec voltage steps to +140, +120 and +100 mV, and at a $[Mg^{2+}]_o$ of 1, 15, 30 and 60 mM, respectively. As seen, the rate as well as the magnitude of current deactivation were increased with increasing

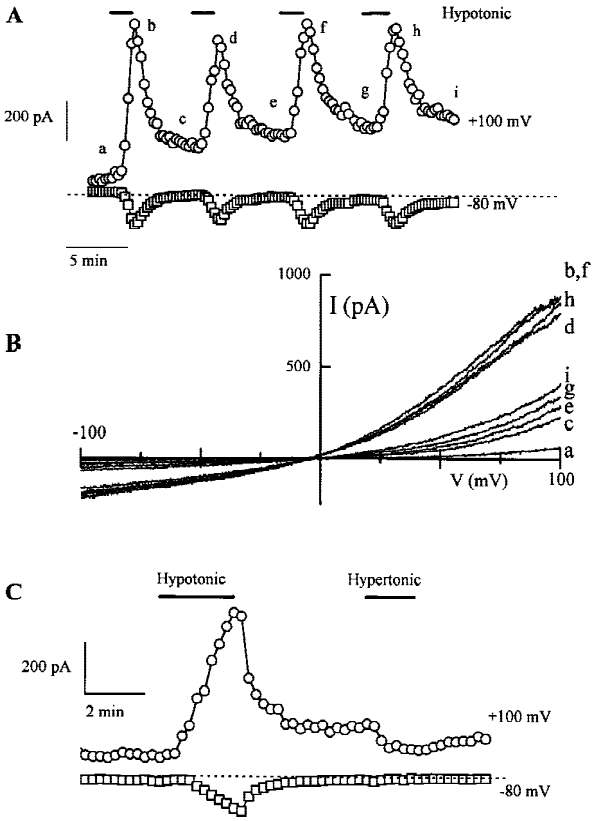

Fig. 4. Repetitive activation of an outwardly rectifying current by cell swelling. The $[Ca^{2+}]_i$ was buffered at 25 nM using 10 mM BAPTA. The isotonic bath solution was a modified Krebs solution containing mannitol. The 27% hypotonic solution was prepared by omitting the relevant amount of mannitol (*see* Materials and Methods). (*A*) Time course of the volume activated current. Linear ramp protocols were applied every 15 sec, and periods of hypotonic exposure were as indicated by the horizontal bar. Data points were calculated as the average current measured in a small window around +100 mV (open circles) and −80 mV (closed circles), respectively. It may be noted that the increased baseline current during the course of the experiment is likely to be due to incomplete cell shrinkage between hypotonic exposures (compare with panel *C*). (*B*) Same cell as in *A*. *IV* relationships reconstructed from the voltage ramps at various time points as indicated in *A*. The figure is representative of experiments on 5 cells under similar conditions. (*C*) Time course of the current measured at +100 mV (open circles) and −80 mV (closed circles) under hypertonic, isotonic and hypotonic conditions. Voltage protocol as in *A*. The figure is representative of experiments on 4 cells under similar conditions.

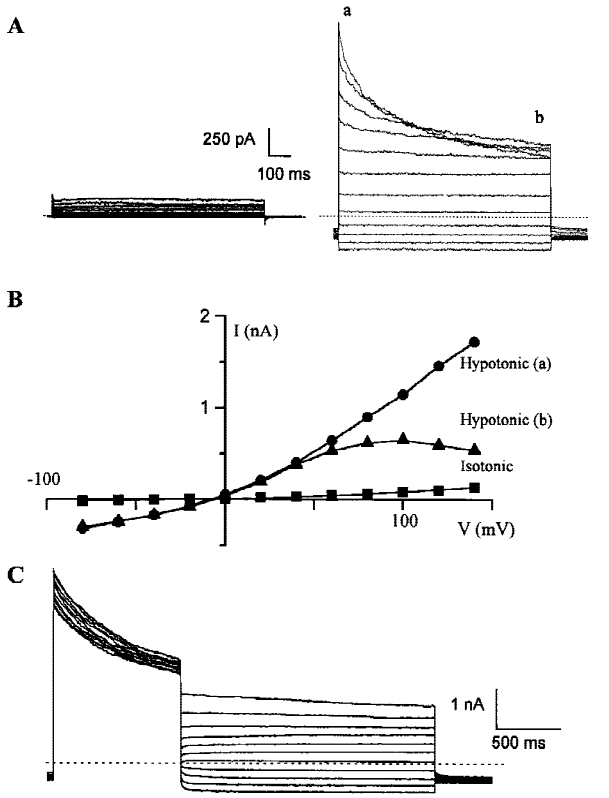

Fig. 5. Voltage-dependent properties of the volume-activated current. (*A*) Whole cell Cl^- currents obtained under isotonic conditions and after exposure of the cell to a 27% hypotonic solution. The voltage protocol was as described in Fig. 1*A*. Note the time-dependent inactivation of the current at depolarized potentials, and the absence of tail currents upon return to the holding potential. (*B*) *IV*-relationships calculated from the current traces shown in *A*, as the average current at each potential, in a narrow window, indicated by the arrows. As seen, the swelling-activated current is strongly outward rectifying at the beginning (*a*), but not at the end (*b*) of the voltage step. (*C*) Current reactivation at hyperpolarized potentials. From a holding potential of −50 mV, the current was inactivated by a 1-sec step to +140 mV, followed by 2-sec steps from +120 to −80 mV, at 20 mV intervals (voltage protocol shown in the insert). The figure is representative of experiments on 8 cells under similar conditions.

$[Mg^{2+}]_o$. Figure 7*B* shows the fractional inactivation of the current, measured at the end of the 1-sec voltage step to +140 mV, as a function of $[Mg^{2+}]_o$.

$I_{Cl,Ca}$ and $I_{Cl,vol}$: Anion Selectivity

To further characterize and compare $I_{Cl,Ca}$ and $I_{Cl,vol}$, we examined the relative permeabilities of these channels to various anions. Following activation of $I_{Cl,Ca}$ or $I_{Cl,vol}$, respectively, the bath solution was replaced for brief time intervals (3–6 ramps) with solutions in which Cl^- was replaced with I^-, gluconate or aspartate (only $I_{Cl,Ca}$) in equimolar amounts. The current was monitored using the linear voltage ramp protocol (*see* Materials and Methods). Figure 8*A* ($I_{Cl,Ca}$) and *B* ($I_{Cl,vol}$) shows *IV* curves reconstructed from the linear voltage ramps. For both $I_{Cl,Ca}$ and $I_{Cl,vol}$, replacing the bath solution by a solution in which Cl^- was substituted by I^- resulted in an increase in the current amplitude measured at positive potentials, and a shift in V_{rev} towards more negative potentials, reflecting a larger permeability of I^- as compared to Cl^-. In contrast, replacing Cl^- with either aspartate or gluconate resulted in a decrease in current

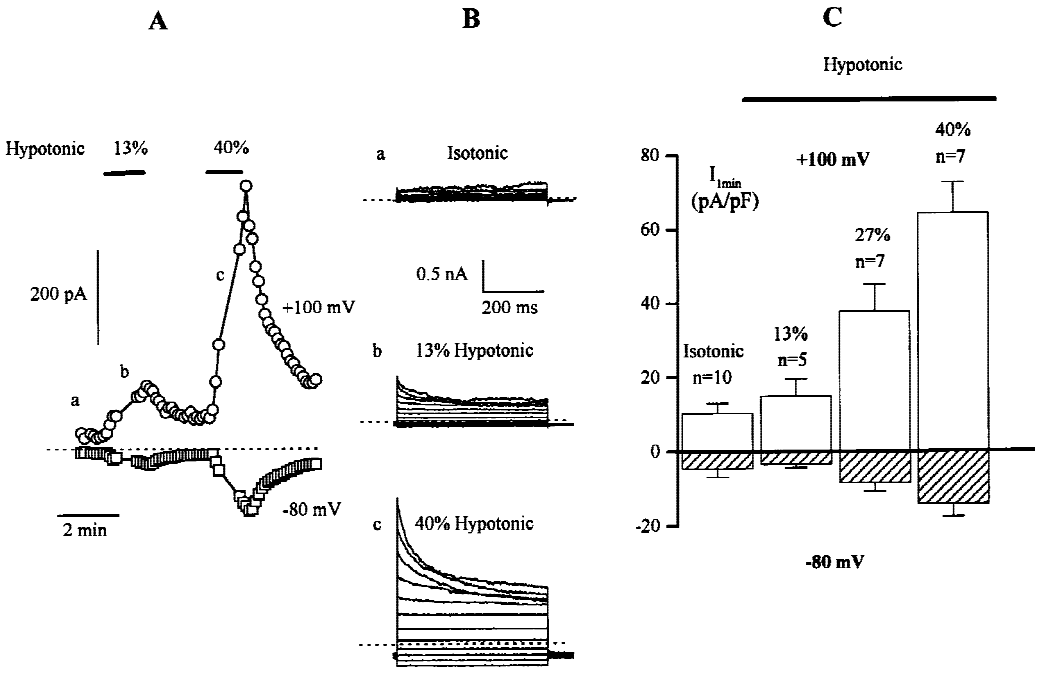

Fig. 6. Dependence of the swelling-activated current on the magnitude of the hypotonic challenge. (*A*) Time course of development of the swelling-induced current under various osmotic conditions. The linear voltage ramp protocol was applied every 15 sec, and hypotonic challenges of varying magnitudes were applied as indicated by the horizontal bars. The data points were calculated as the mean current measured in a narrow window at +100 mV and −80 mV, respectively. The figure shown is representative of similar experiments on 10 cells. (*B*) Same cell as in *A*. The voltage protocol was as described in the legend to Fig. 1*A*. The current traces were obtained at the time points indicated in *A*. (*C*) Current density measured at +100 and −80 mV under isotonic conditions and at time 1 min after hypotonic exposure. The data are presented as means ± SEM, with the number of experiments indicated above each column.

amplitude at positive potentials, and a shift of V_{rev} towards more positive potentials. The shifts in V_{rev} resulting from changing the major anion in the bath were used to calculate the permeabilities of the various anions relative to that of Cl^-, using a modified Goldman-Hodgkin-Katz equation (Eq. 2). The anion permeability sequence: P_I:P_{Cl}:$P_{gluconate}$:$P_{aspartate}$ = 2.4 ± 0.13:1:0.54±0.06: 0.32±0.05 (n = 7–17) was obtained for $I_{Cl,Ca}$, while the sequence P_I:P_{Cl}:$P_{gluconate}$ = 1.39 ± 0.040 (n = 10):1 (n = 11):0.50 ± 0.055 (n = 10) was obtained for $I_{Cl,vol}$. Figure 8*D* ($I_{Cl,Ca}$) and *E* ($I_{Cl,vol}$) show the effect on V_{rev} of reducing $[Cl^-]_o$ to 50% or 10% of that present in the standard medium. For both types of currents, reduction of $[Cl^-]_o$ resulting in a reduced magnitude of the outward currents, as well as a shift in V_{rev} toward more positive potentials, suggesting that both currents were carried mainly by Cl^-. Due to the significant permeability to gluconate (substituting for Cl^- in the bath), and aspartate (present in the pipette solution, only evaluated for $I_{Cl,Ca}$), the measured V_{rev} does not follow that calculated simply based on the Cl^- distribution ratio. However, as seen in Fig. 8*D* and *E*, the experimental data are in good agreement with the values of V_{rev} calculated taking into account the known, relative permeabilities to gluconate and aspartate.

Effect of Cl^- Channel Inhibitors on $I_{Cl,Ca}$ and $I_{Cl,vol}$

The sensitivity of the Ca^{2+}- and swelling-activated currents to various Cl^- channel inhibitors was investigated in a series of experiments summarized in Fig. 9. $I_{Cl,Ca}$ was activated by breaking into the cells with a pipette solution buffered at a $[Ca^{2+}]_i$ of 100 nM, and fast voltage ramps were applied every 15 sec. Figure 9*A* shows the time course of $I_{Cl,Ca}$ measured from these ramps, in a small window at +100 mV, while Fig. 9*B* shows the *IV* relationships generated form the voltage ramps. Niflumic acid (100 μM), a potent blocker of Ca^{2+}-activated Cl^- currents (White & Alwyn, 1990; Nilius et al., 1997*a*) was the most potent of the three inhibitors tested. As seen, application of 100 μM niflumic acid resulted in a fast, reversible inhibition of the current measured at +100 mV. The current inhibition by niflumic acid was calculated at 60% ± 4.5% (n = 12). The commonly used Cl^- channel blockers, 5-Nitro-2-(3-phenylpropylamino)benzoic acid (NPPB, 100 μM) inhibited the Ca^{2+}-activated current measured at +100 mV by 40% ± 3.2% (n = 12). Finally, 4,4′-diisothiocyano-2,2′-stilbenedisulfonic acid (DIDS, 100 μM) caused only 23% ± 3.2% (n = 12) inhibition of the current at +100 mV.

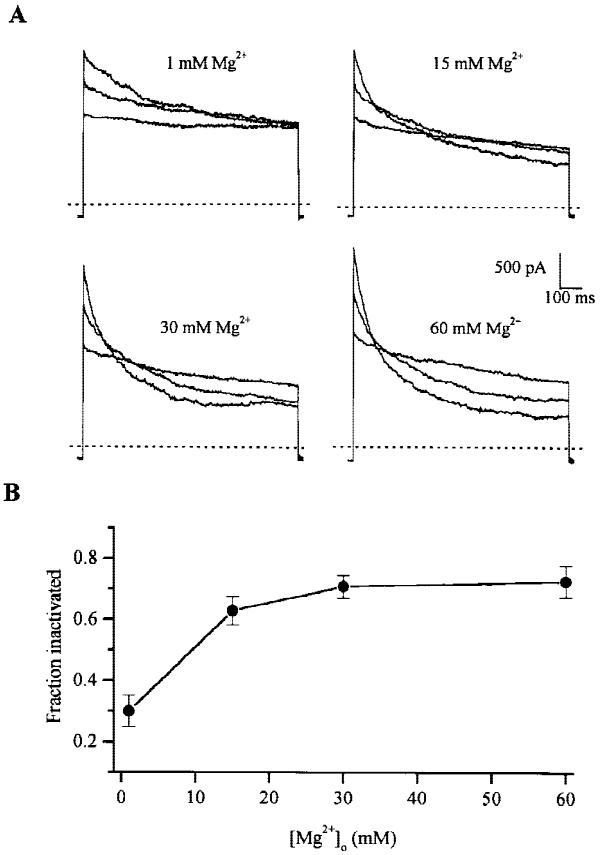

Fig. 7. Effect of extracellular Mg^{2+} on the voltage-dependent inactivation of $I_{Cl,vol}$. (*A*) Voltage-dependent inactivation of $I_{Cl,vol}$ during 1-sec voltage steps to +140, +120 and +100 mV from the holding potential of −50 mV, and at extracellular Mg^{2+} concentrations ($[Mg^{2+}]_o$) of 1, 15, 30 and 60 mM, respectively. The bath Mg^{2+} concentration was increased by replacing NMDG-Cl with $MgCl_2$, in order to maintain $[Cl^-]_o$ constant. The figure shows data from one cell, representative of experiments on 7 cells. (*B*) The fraction of the current inactivated at the end of 1-sec voltage steps to +140 mV as shown in *A*, as a function of $[Mg^{2+}]_o$. The fraction inactivated was calculated by subtracting the mean current in a small interval at the end of the voltage step from the mean current in a similar interval at the start of the voltage step (initial current), and dividing by the initial current. The data are shown as means with SEM error bars ($n = 7$).

Figure 9*C* and *D* shows the effects of niflumic acid (100 μM) and of the anti-estrogen drug, tamoxifen (10 μM), on $I_{Cl,vol}$. Tamoxifen inhibits $I_{Cl,vol}$ in some, but not in all tissues (Nilius et al., 1994*b*). The effects of this drug on $I_{Cl,Ca}$ appear to be variable, hence, tamoxifen (10 μM) completely inhibited $I_{Cl,Ca}$ in bovine pulmonary artery endothelial cells (Nilius et al., 1997*a*), but did not affect $I_{Cl,Ca}$ in T84 colonic carcinoma cells (Valverde, Mintenig & Sepúlveda, 1993). Figure 9*C* shows the time course of $I_{Cl,vol}$, measured at +100 mV, while Fig. 9*D* shows *IV* relationships reconstructed from linear voltage ramps at the times indicated in Fig. 9*C*. At 100 μM, niflumic acid did not affect $I_{Cl,vol}$. In contrast, both the inward and outward current was completely blocked by 10 μM tamoxifen. In fact, in the presence of tamoxifen, the current observed under hypotonic conditions was usually smaller than that seen under isotonic conditions in the absence of tamoxifen, suggesting that the drug also inhibited some component of the background current. It should be noted that the inhibition of $I_{Cl,vol}$ by tamoxifen was not due to cell shrinkage induced by this drug (as assessed by visual inspection of the cells).

Discussion

The Ca^{2+}-activated Current, $I_{Cl,Ca}$

A strongly outwardly rectifying current was activated after an increase in $[Ca^{2+}]_i$ in Ehrlich cells. The mean current density was a saturable function of $[Ca^{2+}]_i$, being virtually zero at +100 mV in BAPTA-loaded cells, and increasing to more than 200 pA/pF at a $[Ca^{2+}]_i$ of 500 nM. At a $[Ca^{2+}]_i$ of 100 nM, which is only slightly higher than the resting level previously measured in these cells (Jørgensen, Lambert & Hoffmann, 1996), a significant activation of $I_{Cl,Ca}$ was already observed. The reversal potential of the Ca^{2+}-activated current shifted with changes in the extracellular Cl^- concentration, suggesting that the current was mainly carried by Cl^-. The anion selectivity sequence, as judged from the shifts in V_{rev} upon bath anion substitution, was $I^- > Cl^- >$ gluconate > aspartate. The current was inhibited by about 60%, 40%, and 20%, respectively, by 100 μM of the Cl^- channel blockers niflumic acid, NPPB and DIDS. These current characteristics are qualitatively similar to those of Ca^{2+}-activated Cl^- currents described in other cell types, including human vascular endothelial cells (Groschner, Graier & Kukovetz, 1994), human umbilical vein endothelial cells (White & Brock, 1994); rat parotid acinar cells (Arreola et al., 1996), calf pulmonary artery endothelial (CPAE) cells (Nilius et al., 1997*a*,*b*), and human leukaemia cells (Sullivan, Kunze & Kroll, 1996).

The kinetics of $I_{Cl,Ca}$ were also investigated. The current exhibited activation at positive potentials, and inactivation at negative potentials, resulting in a strongly outward rectifying steady state current. In contrast, the instantaneous *IV*-relationship was virtually linear. The mechanism of the time dependence of current rectification behaviour is unclear, however, similar observations have been described for the Ca^{2+}-activated Cl^- current in CPAE cells (Nilius et al., 1997*b*) and in rat parotid acinar cells (Arreola et al., 1996). The time course of activation of $I_{Cl,Ca}$ at positive potentials, as well as the time course of deactivation of the current at negative potentials were well fitted by a double exponential function. The fast time constant of current activation was voltage- and $[Ca^{2+}]_i$-dependent, decreasing with increasing magnitude of the applied potentials, as well as with increasing $[Ca^{2+}]_i$. In contrast, the fast time constant of deactiva-

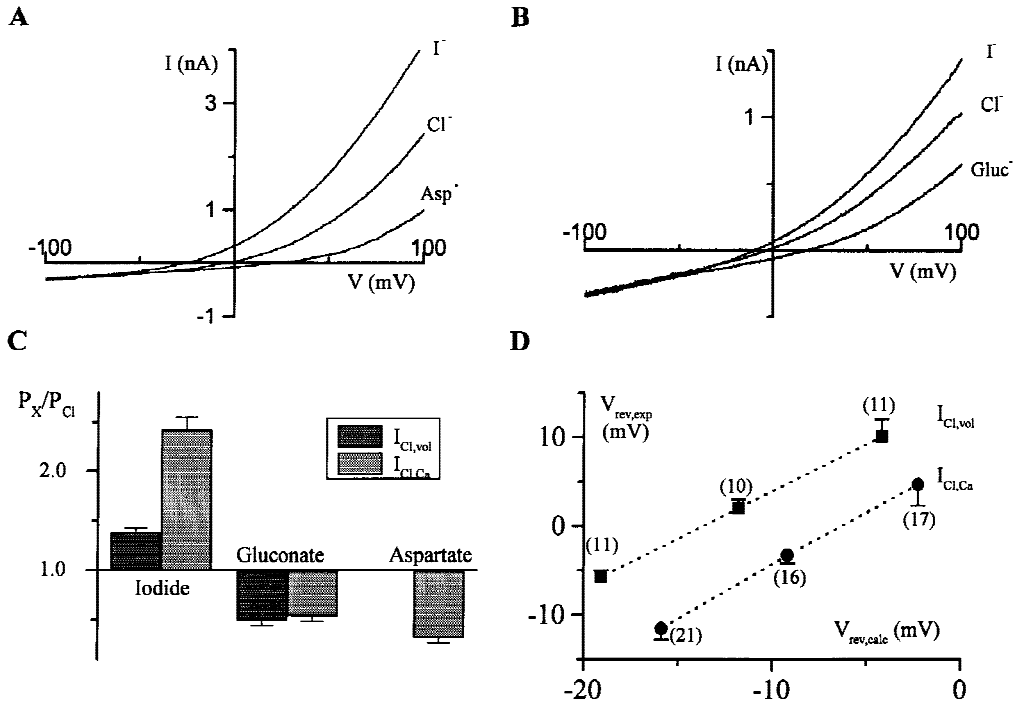

Fig. 8. $I_{Cl,Ca}$ and $I_{Cl,vol}$: Anion selectivity and dependence on $[Cl^-]_o$ *A* ($I_{Cl,Ca}$) and *B* ($I_{Cl,vol}$): Representative *IV* relationships obtained with various anions as the major anion in the bath. $I_{Cl,Ca}$ was activated by breaking into the cell with a pipette solution containing 100 nM free Ca^{2+}. $I_{Cl,vol}$ was activated by exposing the cells to a 27% hypotonic bath solution. A bath concentration of 14.5 mM ($I_{Cl,Ca}$) or 11 mM ($I_{Cl,vol}$) Cl^- was maintained, and an agar bridge bath electrode was used in order to minimize current drift resulting from changes in the bath Cl^- concentration. During brief time periods (3–6 ramps), the normal bath solution was replaced with solutions in which Cl^- was substituted by either iodide, gluconate, or aspartate. Linear voltage ramps were applied every 15 sec, and the *IV* relationships were reconstructed from the voltage ramps. The data represent 10–11 experiments for each condition for both currents. (*C*) Permeability of the Ca^{2+}- and swelling-activated channels to various anions. The permeability ratios, P_X/P_{Cl}, were calculated from the shifts in current reversal potential induced by altering the anionic composition of the bath solution (Eq. 2). The data are shown as mean ± SEM of data from 10–11 cells at each condition. (*D*) Dependence of V_{rev} on $[Cl^-]_o$. The experimental conditions were as in *A* and *B*, respectively. The V_{rev} at each $[Cl^-]_o$ was calculated using Eq. 3, taking into account the relative permeability to gluconate (the anion substituted for Cl^- in the bath), and to aspartate ($I_{Cl,Ca}$, present in the pipette). Note that the reversal potentials shown are the original data, and have not been corrected for junction potential. The relevant $[Cl^-]_o$ is indicated above each data point. Note that V_{rev} shifts to more positive values as $[Cl^-]_o$ is lowered, consistent with a major part of the current being carried by Cl^-. The number of experiments at each $[Cl^-]_o$ is given in parenthesis.

tion of the fully activated current appeared to be largely voltage- and $[Ca^{2+}]_i$ independent. These characteristics are in good agreement with previous data from CPAE cells (Nilius et al., 1997*b*).

Thus, the present results demonstrate that in Ehrlich cells, an increase in $[Ca^{2+}]_i$ activates a Cl^- current which exhibits a very high degree of similarity to Ca^{2+}-activated Cl^- currents previously described in other tissues. This strongly suggests that the Ca^{2+}-activated Cl^--channel, which we have described in the Ehrlich cell, belongs to a family of Ca^{2+}-activated Cl^--channels with very similar properties. Single channel studies in Ehrlich cells have suggested the presence of three or four types of Cl^- channels: ''mini'' 2–7 pS channels, activated by cell swelling; 2–7 pS channels activated by a Ca^{2+} ionophore in intact cells (*see below*); ''medium'' 34 pS channels, the dependence of which on Ca^{2+} was not reported, and finally ''maxi'' 400 pS channels, which were not dependent on Ca^{2+} (Christensen & Hoffmann, 1992). The swelling-activated ''mini'' Cl^- channel could not be activated by Ca^{2+} in isolated patches. However, the Ca^{2+}-ionophore A73122 activated a 2–7 pS Cl^- channel in intact cells. From the single channel measurements it was not possible to determine whether this was an indirect activation of $I_{Cl,vol}$, or whether the Cl^- channel activated by A73122 was a separate, Ca^{2+}-activated channel (Christensen & Hoffmann, 1992). In comparison, the single channel conductance of $I_{Cl,Ca}$ is reported at about 3 pS under physiological conditions in CPAE cells (Nilius et al., 1997*b*), and at 25–30 pS in tracheal epithelial cells (Cunningham et al., 1995).

Possible Physiological Roles of $I_{Cl,Ca}$ in Ehrlich Cells

The density of $I_{Cl,Ca}$ in Ehrlich cells is substantial (~100 pA/pF at a holding potential of +100 mV and a $[Ca^{2+}]_i$ of

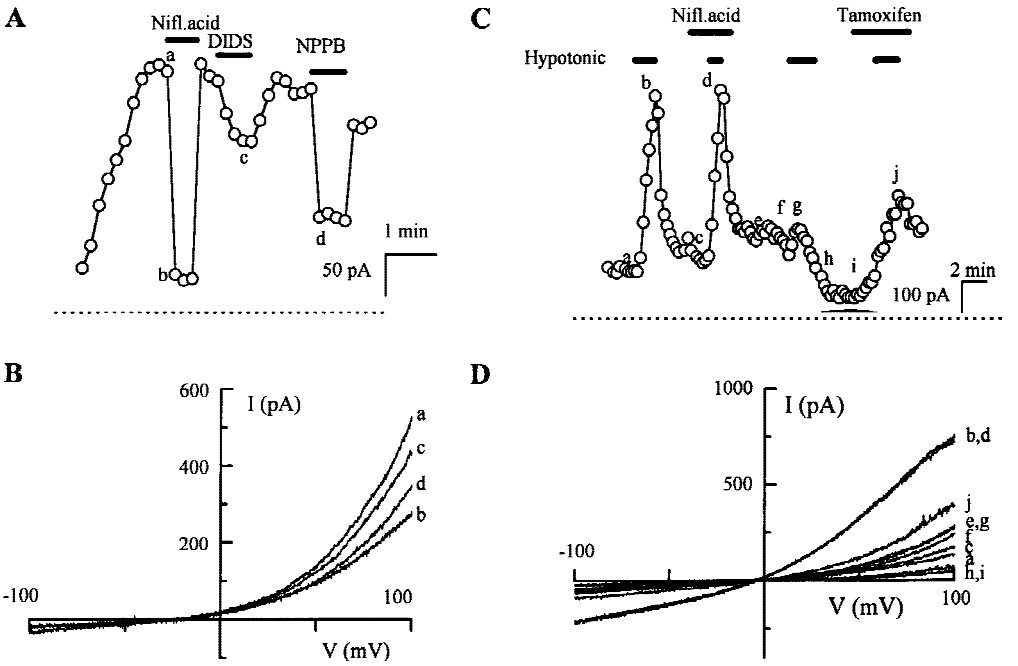

Fig. 9. Effects of inhibitors of Cl^- channels on $I_{Cl,Ca}$ and $I_{Cl,vol}$. (*A*) $I_{Cl,Ca}$: Time course of the current measured at +100 mV. The pipette solution contained 100 nM free Ca^{2+}. Linear voltage ramps were applied every 15 sec, and the current was measured in a small window at +100 mV. Where indicated, the normal bath solution (a modified Krebs solution containing 130 mM NMDG-Cl, 10 mM NaCl and 0 mM KCl) was replaced with solutions containing 100 μM niflumic acid, 100 μM NPPB, or 100 μM DIDS, respectively. (*B*) $I_{Cl,Ca}$: Same cell and conditions as in *A*. The current-voltage relations were reconstructed from the voltage ramps. The percent inhibition of $I_{Cl,Ca}$ by the Cl^- channel blockers, calculated from the voltage ramp experiments using Eq. 1, was 60% ± 4.5% (niflumic acid), 40% ± 3.2% (NPPB), and 23% ± 3.2% (DIDS). The data are given as means ± SEM ($n = 12$ for each drug). (*C*) $I_{Cl,vol}$: Time course of the current activated by exposure to 27% hypotonic solution, in the presence and absence of tamoxifen (10 μM) and niflumic acid (100 μM), respectively. Voltage protocol as in *A*. (*D*) $I_{Cl,vol}$: Same cell as in *C*. Current-voltage relationships were constructed at the time points indicated in *C*, from the currents elicited during application of the voltage ramps. The percent inhibition of $I_{Cl,vol}$ exerted by these inhibitors was 76% ± 2.9% (tamoxifen, $n = 7$), and −4.7% ± 22% (niflumic acid, $n = 4$). (Means ± SEM, calculated as described in Materials and Methods).

100 nM), compared to typical densities reported in other cell types (10–30 pA/pF at a holding potential of +100 mV, *see* Nilius et al., 1997*c*). Thus, it appears likely that $I_{Cl,Ca}$ could play a major functional role in these cells. It may also be noted that the high current density could make Ehrlich cells a useful tool in the investigation of the molecular nature of $I_{Cl,Ca}$. The Ca^{2+}-induced activation of a Cl^- conductance has been suggested to be involved in numerous physiological processes. These include fluid secretion and cell volume changes in salivary gland epithelial cells (Foskett & Melvin, 1989); ACTH secretion in a mouse pituitary tumor cell line (Heisler, 1991), and, in Ehrlich cells, agonist-induced cell shrinkage (Hoffmann, 1993) and concomitant activation of the Na^+,K^+,2Cl^- cotransport system and a Na^+/H^+ exchanger (Jensen, Jessen & Hoffmann, 1993; Pedersen, Jørgensen & Hoffmann, 1997). In many cell types, an increase in $[Ca^{2+}]_i$ can be observed after cell swelling, and in some cells, the RVD process seems to involve Ca^{2+}-activated Cl^- currents (for a review, *see* Hoffmann & Dunham, 1995). In Ehrlich cells, a detectable increase in bulk $[Ca^{2+}]_i$ can only be detected in a fraction (6%) of the swollen cells, and is not required for the RVD process (Jørgensen et al., 1997). However, the present data demonstrate that only a slight increase in $[Ca^{2+}]_i$ is required for activation of $I_{Cl,Ca}$ in these cells. Hence, it is still possible that a localized increase in $[Ca^{2+}]_i$ and activation of $I_{Cl,Ca}$ may contribute to some extent to the RVD response in Ehrlich cells. In any case, a rise in $[Ca^{2+}]_i$ induced by other means, e.g., by stimulation with a Ca^{2+}-mobilizing agonist, during hypotonic exposure, will dramatically increase the rate of the RVD response in these cells (*see* Hoffmann & Dunham, 1995).

THE SWELLING-ACTIVATED CURRENT, $I_{Cl,vol}$

A moderately outward rectifying current was activated 1–2 min after onset of a hypotonic challenge, in Ehrlich cells in which $[Ca^{2+}]_i$ was buffered at 25 nM using BAPTA. The rate of current activation was dependent on the magnitude of the hypotonic challenge, and the current could be reduced by exposing the cells to hypertonic conditions. Together, this strongly suggests that

the current was activated by cell swelling. The current could be repetitively activated by hypotonic exposure. In a study comparing the swelling-activated anion currents in various cell types, a similar pattern of repetitive current activation was found in HeLa cells and in KB3 cells (a human epitheloid cancer cell line), while in rat RBL-2H3 cells, the current could frequently be activated only once (Nilius et al., 1994*b*). The present study demonstrates that $I_{Cl,vol}$ could be activated in cells in which $[Ca^{2+}]_i$ was buffered at 25 nM using BAPTA. Since the resting $[Ca^{2+}]_i$ in Ehrlich cells is about 59 nM (Jørgensen et al., 1996), an increase in $[Ca^{2+}]_i$ is not required for activation of $I_{Cl,vol}$. This is in agreement with the previous observation that RVD in Ehrlich cells is not dependent on an increase in $[Ca^{2+}]_i$ (Jørgensen et al., 1997). Similar results were found in chromaffin cells (Doroshenko & Neher, 1992) and human and bovine vascular endothelial cells (Nilius et al., 1994*a;* Szücs et al., 1996). However, Szücs and coworkers (1996) demonstrated a requirement for a low, permissive $[Ca^{2+}]_i$ for activation of $I_{Cl,vol}$. Some inhibition of RVD has previously been reported in Ca^{2+}-depleted Ehrlich cells. This may reflect a similar requirement, although it should be noted that a permissive $[Ca^{2+}]_i$ for activation of $I_{Cl,vol}$ has not been directly demonstrated in these cells (*see* Hoffmann & Dunham, 1995). The present study shows that $I_{Cl,vol}$ in Ehrlich cells is deactivated in a time- and voltage-dependent manner at depolarized potentials. This is seen in many other cells types, however, the rate and magnitude of current deactivation varies between different cell types, from virtually time- and voltage-independent behavior of $I_{Cl,vol}$ in bovine endothelial cells (Szücs et al., 1996) to very rapid deactivation in C6 glioma cells (Jackson & Strange, 1995) and BC_3H1 cells (Voets et al., 1997). The reason for the voltage-dependent current inactivation is not clear, however, it has been proposed that divalent cations exert an inhibitory effect on $I_{Cl,vol}$ at depolarized potentials (Voets et al., 1997). In agreement with this notion, the present study shows that the rate and magnitude of current inactivation is accelerated by increasing $[Mg^{2+}]_o$. The voltage-dependent current deactivation was well described by a double exponential function, with a fast time constant of about 100–300 msec and a slow time constant of 1–2 sec. Both time constants were voltage-dependent. A slight reactivation of $I_{Cl,vol}$ at hyperpolarized potentials was also observed. Although not further investigated here, the latter type of behavior has been described for swelling-activated anion currents in other cell types, and hence confirms the similarity of the Ehrlich cell $I_{Cl,vol}$ to those observed in other cell types (*see* Strange et al., 1996; Nilius et al., 1996, 1997*b*). The anion permeability sequence of $I_{Cl,vol}$ was $I^- > Cl^- >$ gluconate, a sequence which is consistently found for volume-activated Cl^- channels, with the exception of ClC-2 (*see* Strange et al., 1996; Nilius et al., 1996, 1997*b*). Quantitatively, however, the Ehrlich cell $I_{Cl,vol}$ seems to be unusual in that the relative permeability to gluconate is 0.5, considerably higher than that reported in most other cells. $I_{Cl,vol}$ was completely abolished by the anti-estrogen drug, tamoxifen (10 μM). This compound inhibits the P-glycoprotein (P-gp) involved in multidrug-resistance (MDR), and has been reported to block the putative P-gp-associated Cl^- channel (Mintenig et al., 1994). However, the inhibitory effect of tamoxifen on $I_{Cl,vol}$ may be related to the reported effect of this drug as a calmodulin antagonist (Kirk & Kirk, 1994). The sensitivity of $I_{Cl,vol}$ to tamoxifen varies significantly between tissues (Nilius et al., 1994*b*). This might indicate that $I_{Cl,vol}$ is mediated by different channels in different cell types. However, based on the very similar biophysical properties of this current in different cell types, it appears more likely that the differential effects of tamoxifen reflect cell type specific differences in the regulation of one channel protein. The potent block of $I_{Cl,vol}$ in Ehrlich cells by tamoxifen should provide a powerful tool for investigating the role of this current in the RVD process. In contrast, $I_{Cl,vol}$ was not affected by niflumic acid, which significantly inhibited $I_{Cl,Ca}$ in these cells.

The whole cell characteristics of $I_{Cl,vol}$ in Ehrlich cells are very similar to those reported for volume-activated anion currents in many other tissues, including bovine chromaffin cells (Doroshenko & Neher, 1992), human endothelial cells (Nilius et al., 1994*a*), and human T-lymphocytes (Schumacher et al., 1995). This is intriguing since, in most cell types, swelling-activated efflux of Cl^- and of organic osmolytes is mediated via the same channel (Manolopoulos et al., 1997; *see also* Nilius et al., 1997*b*), while in Ehrlich cells, the dominating part of the Cl^- efflux is probably via a ''mini'' Cl^- channel separate from the taurine channel (Lambert & Hoffmann, 1994; Christensen & Hoffmann, 1992).

The characteristics of $I_{Cl,vol}$ in Ehrlich cells are at variance with those reported for most cloned, putative swelling-activated anion channels (for reviews, *see* Valverde et al., 1995; Jentsch, 1996; Strange et al., 1996; Nilius et al., 1997*b*). Hence, it appears unlikely that the volume-sensitive anion current described in the present study reflects the activity of either of these putative Cl^- channels, and the molecular identity of $I_{Cl,vol}$ in Ehrlich cells requires further investigation.

Comparison of $I_{Cl,Ca}$ and $I_{Cl,vol}$

The present study demonstrates that in Ehrlich cells, two separate Cl^- currents with very different characteristics can be activated by an increase in $[Ca^{2+}]_i$ and by cell swelling, respectively. Thus, physiologically relevant increases in $[Ca^{2+}]_i$ activated a strongly outward rectifying Cl^- current, $I_{Cl,Ca}$. This current was blocked when

increases in $[Ca^{2+}]_i$ were prevented. $I_{Cl,Ca}$ was activated at depolarized potentials and inactivated at hyperpolarized potentials. The anion permeability sequence of $I_{Cl,Ca}$ was $I^- > Cl^- >$ gluconate > aspartate. $I_{Cl,Ca}$ was potently inhibited by the Cl^- channel blocker niflumic acid, and was also sensitive to NPPB, and DIDS. The current kinetics, as well as the current density were voltage- and Ca^{2+}-dependent. Thus, the characteristics of $I_{Cl,Ca}$ strongly resemble those previously described in other cell types. Although a contribution of $I_{Cl,Ca}$ to the RVD process cannot be ruled out based on the present data, this current is clearly different from the volume activated Cl^- current, $I_{Cl,vol}$. This current was activated by cell swelling, was only moderately outward rectifying, and could be fully activated when $[Ca^{2+}]_i$ was buffered below the normal resting value. $I_{Cl,vol}$ was inactivated in a Mg^{2+}-sensitive manner at depolarizing potentials, and reactivated at hyperpolarized potentials. Similar to $I_{Cl,Ca}$, the anion permeability sequence of $I_{Cl,vol}$ was $I^- > Cl^-$ > gluconate, however, $I_{Cl,vol}$ was considerably less permeable to iodide than was $I_{Cl,Ca}$. Finally, $I_{Cl,vol}$ was unaffected by niflumic acid, but was potently inhibited by tamoxifen.

This work was supported by the Danish National Research Council (E.K. Hoffmann), by the F.W.O. Flanders (G.0237.95.N to B. Nilius) and a grant of the European Community (BMH4-CT96-0602, B. Nilius). The authors wish to thank Drs. F.V. Sepúlveda and F. Jørgensen for helpful discussions.

References

Anderson, J.W., Jirsch, J.D., Fedida, D. 1995. Cation regulation of anion current activated by cell swelling in two types of human epithelial cancer cells. *J. Physiol.* **483:**549–557

Arreola, J., Melvin, J.E., Begenisich, T. 1996. Activation of calcium-dependent chloride channels in rat parotid acinar cells. *J. Gen. Physiol.* **108:**35–47

Christensen, O., Hoffmann, E.K. 1992. Cell swelling activates K^+ and Cl^- channels as well as nonselective, stretch-activated cation channels in Ehrlich ascites tumor cells. *J. Membrane Biol.* **129:**13–26

Cliff, W.H., Frizzell, R.A. 1990. Separate Cl^- conductances activated by cAMP and Ca^{2+} in Cl^- secreting epithelia. *Proc. Natl. Acad. Sci. USA* **87:**4956–4960

Cunningham, S.A., Awayda, M.S., Bubien, J.K., Ismailov, I.I., Arrate, M.P., Berdiev, B.K., Benos D.J., Fuller, C.M. 1995. Cloning of an epithelial chloride channel from bovine trachea. *J. Biol. Chem.* **270:**31016–31026

Doroshenko, P., Neher, E. 1992. Volume-sensitive chloride conductance in bovine chromaffin cell membrane. *J. Physiol.* **449:**197–218

Foskett, J.K., Melvin, J.E. 1989. Activation of salivary secretion: Coupling of cell volume and $[Ca^{2+}]_i$ in single cells. *Science* **244:**1582–1585

Groschner, K., Graier, W.F., Kukovetz, W.R. 1994. Histamine induces K^+, Ca^{2+}, and Cl^- currents in human vascular endothelial cells — Role of ionic currents in stimulation of nitric oxide biosynthesis. *Circ. Res.* **75:**304–314

Heisler, S. 1991. Chloride channel blockers inhibit ACTH secretion from mouse pituitary tumor cells. *Am. J. Physiol.* **260:**E505–512

Hoffmann, E.K. 1978. Regulation of cell volume by selective changes in the leak permeabilities of Ehrlich ascites tumor cells. *Alfred Benzon Symp.* **11:**397–417

Hoffmann, E.K. 1993. Control of volume regulatory ion transport processes in mammalian cells: Signalling by second messengers. *Alfred Benzon Symp.* **34:**273–294

Hoffmann, E.K., Dunham, P.B. 1995. Membrane mechanisms and intracellular signalling in cell volume regulation. *Int. Rev. Cytology* **161:**173–262

Hoffmann, E.K., Lambert, I.H., Simonsen, L.O. 1986. Separate, Ca^{2+}-activated K^+ and Cl^- transport pathways in Ehrlich ascites tumor cells. *J. Membrane Biol.* **91:**227–244

Jackson, P.S., Strange, K. 1995. Characterization of the voltage-dependent properties of a volume-sensitive anion conductance. *J. Gen. Physiol.* **105:**661–677

Jensen, B.S., Jessen, F., Hoffmann, E.K. 1993. Na^+, K^+, Cl^- cotransport and its regulation in Ehrlich ascites tumor cells. Ca^{2+}/Calmodulin and Protein kinase C dependent pathways. *J. Membrane Biol.* **131:**161–178

Jentsch, T.J. 1996. Chloride channels: a molecular perspective. *Curr. Op. Neurobiol.* **6:**303–310

Jørgensen, N.K., Christensen, S., Harbak, H., Brown, A.M., Lambert, I.H., Hoffmann, E.K., Simonsen, L.O. 1997. On the role of Ca^{2+} in regulatory volume decrease in Ehrlich ascites tumor cells. *J. Membrane Biol.* **157:**281–299

Jørgensen, N.K., Lambert, I.H., Hoffmann, E.K. 1996. Role of LTD_4 in the regulatory volume decrease response in Ehrlich ascites tumor cells. *J. Membrane Biol.* **151:**159–173

Kirk, J., Kirk, K. 1994. Inhibition of volume-activated I- and taurine efflux from HeLa cells by P-glycoprotein blockers correlates with calmodulin inhibition. *J. Biol. Chem.* **269:**29389–29394

Lambert, I.H., Hoffmann, E.K. 1994. Cell swelling activates separate taurine and chloride channels in Ehrlich mouse ascites tumor cells. *J. Membrane Biol.* **142:**289–298

Lambert, I.H., Hoffmann, E.K., Jørgensen, F. 1989. Membrane potential, anion and cation conductances in Ehrlich ascites tumor cells. *J. Membrane Biol.* **111:**113–132

Manolopoulos V.G., Voets T., Declercq, P.E., Droogmans G., Nilius B. 1997. Swelling-activated efflux of taurine and other osmolytes in endothelial cells. *Am. J. Physiol.* **273:**C214–C222

Mintenig, G.M., Valverde, M.A., Sepulveda, F.V., Gill, D.R., Hyde, S.C., Higgins, C.F. 1994. Specific inhibitors distinguish the chloride channel and drug transporter functions associated with the human multidrug resistance P-glycoprotein. *Receptor Channels* **1:**305–313

Neher, E. 1992. Correction for liquid junction potentials in patch clamp experiments. *Meth. Enzymol.* **207:**123–131

Nilius, B., Eggermont, J., Voets, T., Buyse, G., Manopoulos, V., Droogmans, G. 1997*d.* Properties of volume-regulated anion channels in mammalian cells. *Prog. Biophysics Mol. Biol.* **64:** (*in press*)

Nilius, B., Eggermont, J., Voets, T., Droogmans, G. 1996. Volume-activated Cl^--channels. *Gen. Pharmacol.* **27:**1131–1140

Nilius, B., Oike, M., Zahradnik, I., Droogmans, G. 1994*a.* Activation of a Cl-current by hypotonic volume increase in human endothelial cells. *J. Gen. Physiol.* **103:**787–805

Nilius, B., Prenen, J., Szucs, G., Wei, L., Tanzi, F., Voets, T., Droogmans, G. 1997*a.* Calcium-activated chloride channels in bovine pulmonary artery endothelial cells. *J. Physiol.* **498.2:**381–396

Nilius, B., Prenen, J., Voets, T., Van den Bremt, K., Eggermont, J., Droogmans, G. 1997*b.* Kinetic and pharmacological properties of the calcium-activated chloride-current in macrovascular endothelial cells. *Cell Calcium* **22:**53–63

Nilius, B., Sehrer, J., Viana, F., De Greef, C., Raeymaekers, L., Eggermont, J., Droogmans. 1994*b*. Volume-activated Cl^- currents in different mammalian non-excitable cell types. *Pfluegers Arch.* **428:**364–371

Nilius, B., Viana, F., Droogmans, G. 1997*c*. Ion channels in vascular endothelium. *Annu. Rev. Physiol.* **59:**145–170

Pedersen, S.F., Jørgensen, N.K., Hoffmann, E.K. 1997. Dynamics of $Ca^{2+}{}_i$ and pH_i in Ehrlich ascites tumor cells after hypertonic challenge of Ca^{2+} mobilizing agonists. *Am. J. Physiol.*, (*in press*)

Schumacher, P.A., Sakellaropoulos, D.J., Phipps, D.J., Schlichter, L.C. 1995. Small-conductance chloride channels in human peripheral T lymphocytes. *J. Membrane Biol.* **145:**217–232

Stoddard, J.S., Steinbach, J.H., Simchowitz, L. 1993. Whole cell Cl^- currents in human neutrophils induced by cell swelling. *Am. J. Physiol.* **265:**C156–C165

Strange, K., Emma, F., Jackson, P.S. 1996. Cellular and molecular physiology of volume-sensitive anion channels. *Am. J. Physiol.* **270:**C711–C730

Sullivan, R., Kunze, D.L., Kroll, M.H. 1996. Thrombin receptors activate potassium and chloride channels. *Blood* **87:**648–656

Szücs, G., Heinke, S., Droogmans, G., Nilius, B. 1996. Activation of the volume-sensitive chloride current in vascular endothelial cells requires a permissive intracellular Ca^{2+} concentration. *Pfluegers Arch.* **431:**467–469

Valverde, M.A., Hardy, S.P., Sepúlveda, F.V. 1995. Chloride channels: a state of flux. *FASEB J.* **9:**509–515

Valverde, M.A., Mintenig, G.M., Sepúlveda, F.V. 1993. Differential effects of tamoxifen and I^- on three distinguishable chloride currents activated in T84 cells. *Pfluegers Arch.* **425:**552–554

Voets, T., Droogmans, G., Nilius, B. 1997. Modulation of voltage-dependent properties of a swelling-activated Cl^--current. *J. Gen. Physiol.* **110:**313–325

Wang, Y., Roman, R., Lidofsky, S.D., Fitz, J.G. 1996. Autocrine signalling through ATP release represents a novel mechanism for cell volume regulation. *Proc. Natl. Acad. Sci. USA* **93:**12020–12025

Wang, Z., Mitsuiye, T., Rees, S.A., Noma, A. 1997. Regulatory volume decrease of cardiac myocytes induced by β-adrenergic activation of the Cl^- channel in guinea pig. *J. Gen. Physiol.* **110:**73–82

White, M.M., Alwyn, M. 1990. Niflumic and flufenamic acid are potent reversible blockers of Ca^{2+}-activated Cl^- channels in *Xenopus* oocytes. *Molecular Pharmacology* **37:**720–724

White, C.R., Brock, T.A. 1994. Calcium-mobilizing agonists stimulate anion fluxes in cultured endothelial cells from human umbilical vein. *J. Membrane Biol.* **142:**171–179